Ther Adv Neurol Disord
2018, Vol. 11: 1–11
DOI: 10.1177/1756286418759974

High-resolution nerve ultrasound and magnetic resonance neurography as complementary neuroimaging tools for chronic inflammatory demyelinating polyneuropathy

Kalliopi Pitarokoili, Moritz Kronlage, Philip Bäumer, Daniel Schwarz, Ralf Gold, Martin Bendszus and Min-Suk Yoon

Abstract

Background: We present a clinical, electrophysiological, sonographical and magnetic resonance neurography (MRN) study examining the complementary role of two neuroimaging methods of the peripheral nervous system for patients with chronic inflammatory demyelinating polyneuropathy (CIDP). Furthermore, we explore the significance of cross-sectional area (CSA) increase through correlations with MRN markers of nerve integrity.

Methods: A total of 108 nerve segments on the median, ulnar, radial, tibial and fibular nerve, as well as the lumbar and cervical plexus of 18 CIDP patients were examined with high-resonance nerve ultrasound (HRUS) and MRN additionally to the nerve conduction studies.

Results: We observed a fair degree of correlation of the CSA values for all nerves/nerve segments between the two methods, with a low random error in Bland–Altman analysis (bias = HRUS-CSA – MRN-CSA, –0.61 to –3.26 mm). CSA in HRUS correlated with the nerve T2-weighted (nT2) signal increase as well as with diffusion tensor imaging parameters such as fractional anisotropy, a marker of microstructural integrity. HRUS-CSA of the interscalene brachial plexus correlated significantly with the MRN-CSA and nT2 signal of the L5 and S1 roots of the lumbar plexus.

Conclusions: HRUS allows for reliable CSA imaging of all peripheral nerves and the cervical plexus, and CSA correlates with markers of nerve integrity. Imaging of proximal segments as well as the estimation of nerve integrity require MRN as a complementary method.

Keywords: chronic inflammatory demyelinating polyneuropathy, high-resolution ultrasound, magnetic resonance neurography, nerve conduction studies, peripheral neuropathy

Received: 3 November 2017; revised manuscript accepted: 24 January 2018.

Correspondence to:
Kalliopi Pitarokoili
Department of Neurology, Ruhr University, St. Josef Hospital, Gudrunstr. 56, 44791, Bochum, Germany
Kalliopi.Pitarokoili@ruhr-uni-bochum.de

Ralf Gold
Min-Suk Yoon
Department of Neurology, St. Josef Hospital, Ruhr University Bochum, Germany

Moritz Kronlage
Philip Bäumer
Daniel Schwarz
Martin Bendszus
Heidelberg University Hospital, Department of Neuroradiology, Heidelberg, Germany

Introduction

The use of neuroimaging for the diagnosis of chronic inflammatory demyelinating polyneuropathy (CIDP) is becoming increasingly important. However, the discrepancy of the role of neuroimaging for diagnosis and treatment monitoring between autoimmune diseases of the central and peripheral nervous system is still striking. For multiple sclerosis, dissemination of T2 lesions in magnetic resonance imaging (MRI) in space supports clinical diagnosis, whereas MRI alone can ensure early diagnosis in the context of dissemination of the lesions in time.[1] On the other hand, enlargement of proximal segments of peripheral nerves or gadolinium enhancement of the brachial or lumbosacral plexus in magnetic resonance neurography (MRN) is only a supportive

criterion for CIDP diagnosis according to the European Federation of Neurological Societies' guidelines (level C recommendation).[2]

Numerous studies show T2 alterations of peripheral nerves in MRN as well as a CSA increase of peripheral nerves and plexuses in MRN and high-resonance nerve ultrasound (HRUS) for CIDP patients compared to controls.[3–9] New MRN biomarkers of axonal and myelin integrity, such as diffusion tensor imaging (DTI) parameters (fractional anisotropy, radial and axial diffusivity), were investigated by our group, whereas their use in treatment monitoring remains to be examined in further longitudinal studies.[10] A future challenge for neuroimaging of the peripheral nervous system is assisting in an early diagnosis and reliable treatment monitoring, which would lead to earlier treatment initiation or escalation.[11–14]

Before these neuroimaging techniques can be introduced into everyday practice, studies comparing their imaging potential and their correlation with clinical parameters, as well as with electrophysiological parameters, as the 'gold standard' are crucial. Therefore, the primary objective of this study was to systematically evaluate the individual role of HRUS and MRN in assessing the morphological alterations of all peripheral nerves and plexus in CIDP. Furthermore, we investigated the significance of cross-sectional area (CSA) increase through correlations with MRN markers of nerve integrity and oedema.

Methods

Patients

This study was approved by the institutional ethics committee (No. 4382-12). The study was conducted in accordance with the ethical standards laid down in the declaration of Helsinki of 1964 and its later amendments. Written informed consent was obtained from all participants. A total of 18 patients from the outpatient clinic (St. Josefs Hospital, Bochum) aged over 18 years, fulfilling the diagnostic criteria of typical CIDP and with severity distributed along the inflammatory neuropathy cause and treatment (INCAT) validated overall disability sum score (ODSS) scale, were recruited over a period of 6 months in the study. Medical Research Council (MRC) values for flexion and extension of the foot and the hand and fingers were documented. For the diagnosis of definite CIDP we used the diagnostic criteria proposed by the Joint Task Force of the European Federation of Neurological Societies and the Peripheral Nerve Society.[13]

Nerve conduction studies

Electrophysiological studies, nerve ultrasound and clinical evaluation were performed over a period of 3 weeks.

All electrophysiological studies were performed by a board-certified neurologist (M-SY) (Medtronic 4 canal electromyography device; Medtronic, Meerbusch, Germany). All testing was done while maintaining the skin temperature at 34°C. Mixed studies (motor, sensory) were performed in the median and ulnar nerve, motor studies in the tibial nerve and sensory studies in the sural nerve. All nerves were examined bilaterally. Sural potentials were recorded after antidromic stimulation at the lower lateral third of the mid-calf, the recording electrode being located below the lateral malleolus. Averaging of at least 10 responses was performed for all sensory studies to improve signal-to-noise ratio. The intrarater reliability of the examiner (M-SY) was determined with the help of the dependability coefficient (φ) after measuring the compound motor action potential (CMAP) and sensory nerve action potential (SNAP) of the median nerve in a single healthy control on five consecutive days. We used the reference values proposed by Stöhr and colleague.[14]

Ultrasound examination

Ultrasonography was performed on the same day as the nerve conduction studies (NCS) by one neurologist (KP) with at least 4 years of neuromuscular ultrasound experience. All ultrasound studies have been performed with the use of an Aplio® XG ultrasound system (Toshiba Medicals, Tochigi, Japan). For the superficial nerves of the lower extremities (fibular nerve at the fibula head, tibial nerve at the ankle, sural nerve), an 18 MHz linear array transducer was used, and for the deeper nerves (tibial and fibular in popliteal fossa) a 12 MHz linear array transducer was used. The transducer was always kept perpendicular to the nerves to avert anisotropy. No additional force was applied other than the weight of the transducer, and the extremities were kept in the neutral position to avoid causing any artificial nerve deformity. CSA measurements were performed at the inner border of the thin hyperechoic epineural rim by the continuous tracing technique, and

the average values were calculated after serially measuring three times.

The maximum CSA of all peripheral nerves and the brachial plexus were measured bilaterally in all CIDP patients at the following sites:

1. median nerve at the entrance to the carpal tunnel (retinaculum flexorum), forearm (approximately 15 cm proximal to the retinaculum flexorum) and upper arm (around the middle of the distance between the medial epicondyle and axillary fossa);
2. ulnar nerve at Guyon's canal, forearm (approximately 15 cm proximal to Guyon's canal), elbow (between medial epicondyle and olecranon), upper arm (around the middle of the distance between the medial epicondyle and axillary fossa);
3. radial nerve in the spiral groove;
4. tibial nerve in the popliteal fossa and at the ankle;
5. fibular nerve at the fibular head and in the popliteal fossa;
6. sural nerve (between the lateral and medial head of the gastrocnemius muscle);
7. the brachial plexus was also assessed in the supraclavicular (next to the subclavian artery) and interscalene space.

MRI technique, image interpretation and MRI outcome measures

HRUS parameters were correlated with MRN biomarkers of nerve morphology (CSA) and DTI. Sequence parameters, postprocessing and interpretation of MRN in correlation with clinical data and electrophysiology in the same cohort have been published separately.[10,15]

Briefly, we used a 3.0 T magnetic resonance scanner (Magnetom TIM-TRIO, Siemens Healthcare, Erlangen, Germany) and acquired a fat-saturated tT2-weighted 3D sequence [sampling perfection with application-optimized contrasts using different flip angle evolution (SPACE)] of the lumbosacral plexus, and a fat-saturated high-resolution T2-weighted turbo spin-echo (TSE) sequence for visualization of nerve morphology and quantification of normalized T2-weighted signal at mid-thigh, the lower leg and the upper arm of one randomly selected side (left/right) as described by Kronlage and colleagues.[10] Moreover, a single-shot spin-echo echo planar imaging (EPI) DTI sequence was acquired at the mid-thigh, the lower leg and the upper arm of one randomly selected side (left/right).

Nerve segmentation was conducted by MK, who has more than 3 years of experience in neuromuscular imaging, using a freehand region-of-interest tool as described by Kronlage and colleagues.[10]

The following nerves were measured with MRN:

1. maximum CSA of the median nerve in the upper arm between 8 cm and 15 cm proximally to the middle of the elbow;
2. maximum CSA of the ulnar nerve in the upper arm between 8 cm and 15 cm proximally to the middle of the elbow (line crossing horizontally through the elbow joint);
3. maximum CSA of the radial nerve at the upper arm between 8 cm and 16 cm proximally to the middle of the elbow (line crossing horizontally through the elbow joint);
4. maximum CSA of the tibial nerve at the thigh (tibial portion of the sciatic nerve), which was between 10 cm and 20 cm proximally to the popliteal fossa as well as at the site of the maximal CSA at the lower leg, which was 8–12 cm distally to the popliteal fossa;
5. maximum fibular nerve CSA at the thigh, which was between 10 cm and 20 cm proximal to the popliteal fossa (fibular portion of the sciatic nerve).

Statistics

Statistical analysis was conducted using Prism 7 (GraphPad Software, La Jolla, USA). All values are shown as mean ± standard deviation (SD) unless stated otherwise; $p < 0.05$ was regarded as statistically significant. The D'Agostino and Pearson normality test was applied to test the distribution of MRN and HRUS data. The Pearson correlation coefficient r was reported for all correlation analyses unless stated otherwise. We applied the nonlinear Spearman's rank correlation coefficient rs for correlations with ODSS and with F-wave latency. For the correlations, the maximum F-wave latency was used for absent F-waves.

In order to assess agreement between HRUS and MRN-CSA measurements, a Bland–Altman plot was used. Mean bias (bias = HRUS-CSA − MRN-CSA) as well as 95% limits of agreement (±1.96 SD of the bias) were depicted as dotted lines in the plot.

To calculate statistical significance between two groups, Student's t test and nonparametrical Mann–Whitney U test were used. A Bonferroni–Holm correction was applied to all electrophysiological and ODSS correlation analyses, and the corrected p values are presented.

Results

A total of 18 CIDP patients (mean age 58.9, SD ± 7.2; seven women) participated in the study and were evaluated with NCS, HRUS and MRN a mean of 4.7 years (SD ± 4.9) after disease onset. Clinical assessment included the INCAT validated ODSS, which combines arm and leg disability in a score ranging from 0 (no signs of disability) to 12 (most severe disability score); the mean ODSS ± SD (min. – max.) was 3.1 ± 1.42 (min. – max., 1–6) for this cohort.[11] Overall, 13 patients received intravenous immunoglobulins and five additional immunosuppressive escalating treatments (Supplementary Table 1) at this time point of the study.

Correlations of quantitative parameters of HRUS and MRN

Median nerve

MRN values correlated significantly with HRUS values (Figure 1; $p = 0.002$, $r = 0.73$, $n = 15$). The Bland–Altman plot showed a negative mean bias (bias = HRUS-CSA − MRN-CSA) of −2.447 (SD of the bias 6.126) and the 95% limits of agreement (±1.96 SD of the bias) at −14.45 and 9.560. These results indicate a fair degree of correlation between the two methods for the estimation of the maximum CSA of the upper arm, with the CSA measured by MRN being more frequently higher than the CSA measured by HRUS.

Mean normalized nerve T2-weighted signal (nT2) did not correlate with HRUS-CSA values ($p = 0.11$, $r = 0.41$, $n = 16$).

Interestingly, the fractional anisotropy values of DTI correlated significantly with the HRUS-CSA ($p = 0.0002$, $r = -0.87$, $n = 12$) of the median nerve in the upper arm.

HRUS-CSA values correlated significantly with conduction velocity of the median nerve (CV) after stimulation from elbow to abductor pollicis brevis ($p < 0.0001$, $r = -0.85$, $n = 17$) but not with the proximal CMAP ($p = 0.08$, $r = -0.34$, $n = 17$).

HRUS-CSA values measured in the forearm also correlated significantly with the conduction velocity of the median nerve ($p = 0.02$, $r = -0.54$, $n = 17$).

HRUS-CSA values measured in the entrance to the carpal tunnel did not correlate with any electrophysiological parameter.

Ulnar nerve

MRN values correlated significantly with HRUS values (Figure 1; $p = 0.0026$, $r = 0.7178$, $n = 15$) The Bland–Altman plot showed a negative mean bias (bias = HRUS-CSA − MRN-CSA) of −1.607 (SD of the bias 2.859) and the 95% limits of agreement (±1.96 SD of the bias) at −7.211 and 3.998. These results indicate a fair degree of correlation between the two methods for the estimation of the maximum ulnar CSA of the upper arm, with the CSA measured by MRN being more frequently higher than the CSA measured by HRUS.

nT2 signal correlated significantly with the HRUS-CSA values ($p = 0.003$, $r = 0.72$, $n = 15$), however, fractional anisotropy (FA) values did not correlate with HRUS-CSA ($p = 0.05$, $r = -0.56$, $n = 12$).

HRUS-CSA, as well as MRN-CSA, values did not correlate with any electrophysiological parameter (Table 1). HRUS-CSA values measured in Guyon's canal, forearm and elbow did not correlate with any electrophysiological parameters of the ulnar nerve.

Radial nerve

MRN values correlated significantly with HRUS values (Figure 1; $p = 0.0023$, $r = 0.7372$, $n = 15$). The Bland–Altman plot showed a negative mean bias (bias = HRUS-CSA − MRN-CSA) of −0.6133 (SD of the bias 3.055) and the 95% limits of agreement (±1.96 SD of the bias) at −6.601 and 5.374. These results indicate a fair degree of correlation between the two methods for the estimation of the maximum radial CSA of the upper arm, with the CSA measured by MRN being more frequently higher than the CSA measured by HRUS.

nT2 signal did not correlate significantly with HRUS-CSA values of the radial nerve at the upper arm ($p = 0.69$, $r = -089$, $n = 15$).

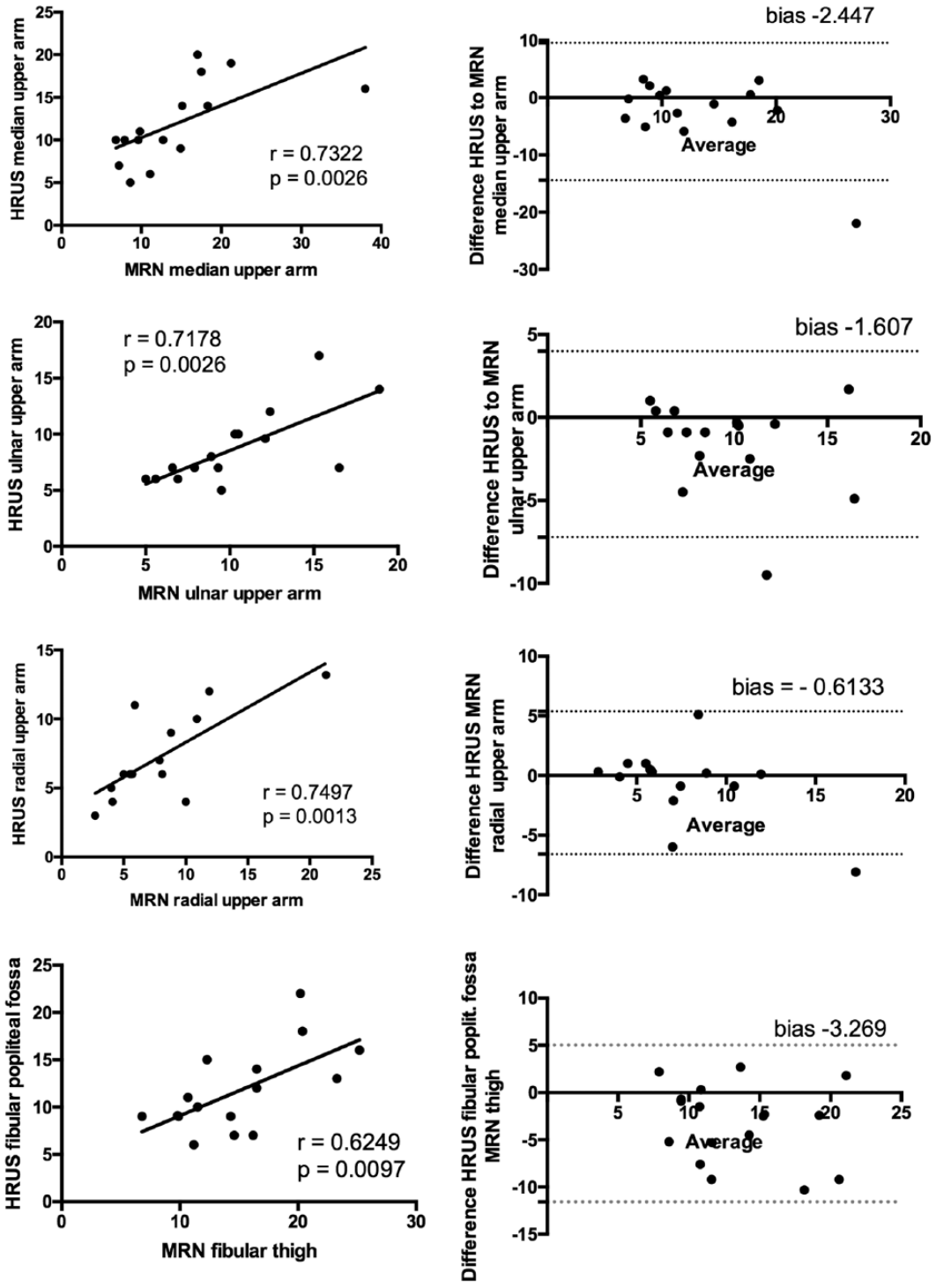

Figure 1. Correlations between CSA in MRN and HRUS (all values in mm^2) and Bland–Altmann plots for the median, ulnar and radial nerve in the upper arm and the fibular nerve.
HRUS-CSA values for all nerves correlated with MRN values for all nerves measured (right side). The Bland–Altman plots (left side) show a negative mean bias (bias = HRUS-CSA – MRN-CSA) between –0.6 and –3.2. These results indicate a fair degree of correlation between the variables with MRN-CSA values being more frequently higher than HRUS-CSA values. Random error is lower for the radial and higher for the fibular nerve. (a) Dashed line, mean bias in Bland–Altman plots; solid line, ±1.96 SD (95% CI).
CSA, cross-sectional area; HRUS, high-resonance nerve ultrasound; magnetic resonance neurography.

Table 1. Correlations of HRUS and MRN-CSA with electrophysiological parameters (CMAP) and nT2, FA values. For the brachial plexus, correlation analysis has been performed with F-waves of the median nerve and for the lumbar plexus with F-waves from the tibial nerve. Significant correlations are marked.

CSA	CV	CMAP	nT2	FA
HRUS – median	***p* < 0.0001** ***r* = – 0.85, *n* = 17**	$p = 0.08$ $r = -0.34$, n = 17	$p = 0.11$ $r = 0.41$, $n = 16$	***p* = 0.0002** ***r* = –0.87, *n* = 12**
HRUS – ulnar	$p = 0.2$ $r = 0.4$, $n = 9$	$p = 0.4$ $r = 0.2$, $n = 9$	***p* = 0.003** ***r* = 0.72, *n* = 15**	$p = 0.05$ $r = -0.56$, $n = 12$
HRUS – radial	n.a.	n.a.	$p = 0.6$ $r = -089$, $n = 15$	$p = 0.12$ $r = -0.42$, $n = 11$
HRUS – tibial	$p = 0.45$ $r = -0.03$ $n = 15$	$p = 0.23$ $r = -0.17$, $n = 17$	$p = 0.5$ $r = -0.16$, $n = 16$	$p = 0.89$ $r = -0.03$, $n = 18$
HRUS – fibular	n.a.	n.a.	$p = 0.09$ $r = 0.44$, $n = 15$	n.a.
HRUS – brachial plexus	$p = 0.54$ $r = 0.20$, $n = 11$		***p* = 0.023** ***r* = 0.63, *n* = 13**	n.a.

CMAP, compound motor action potential; CSA, cross-sectional area; CV, conduction velocity; FA, fractional anisotropy; HRUS, high-resonance nerve ultrasound; MRN, magnetic resonance neurography; n.a., not applicable; nT2, normalized nerve T2-weighted signal.

FA values did not correlate with HRUS-CSA values ($p = 0.12$, $r = -0.42$, $n = 11$) (Table 1).

Tibial nerve

As depicted in Figure 2, CSA of the tibial nerve gradually increased from distal to proximal segments of the lower extremity (Figure 2).

Although CSA values from the two methods did not correlate with each other, CSA values of the tibial nerve from different segments measured with the same method correlated with each other. More specifically, HRUS-CSA of the tibial nerve at the popliteal fossa correlated significantly with HRUS-CSA at the ankle ($p = 0.0391$, $r = 0.5040$, $r = 17$).

nT2 signal at the thigh did not correlate with HRUS-CSA values at the popliteal fossa ($p = 0.88$, $r = -0.038$, $n = 16$).

nT2 signal at the lower leg did not correlate with HRUS-CSA values at the popliteal fossa ($p = 0.53$, $r = -0.16$, $n = 16$).

HRUS-CSA values did not correlate with any of the electrophysiological parameters of the tibial nerve.

FA values at the thigh did not correlate with HRUS-CSA at the popliteal level ($p = 0.89$, $r = -0.03$, $n = 18$) (Table 1).

Fibular nerve

In this case, HRUS-CSA values of the fibular nerve at the popliteal fossa correlated significantly with MRN-CSA values at the thigh (Figure 1; $p = 0.009$, $r = 0.62$, $n = 16$).

The Bland–Altman plot showed a negative mean bias (bias = HRUS-CSA − MRN-CSA) of −3.269 (SD of the bias 4.231) and the 95% limits of agreement (±1.96 SD of the bias) at −11.56 and 5.025. The degree of correlation between the two methods for the estimation of the maximum fibular CSA of fibular nerve at the lower thigh is not satisfactory, with the CSA measured by MRN being more frequently much higher than the CSA measured by HRUS.

nT2 signal at the thigh did not correlate with HRUS-CSA values at the popliteal fossa ($p = 0.09$, $r = 0.44$, $n = 15$) or fibular head ($p = 0.081$, $r = 0.75$, $n = 17$) (Table 1).

Plexus brachialis: plexus lumbalis

The average of the MRN-CSA of the anterior divisions of the spinal nerves L5 and S1 at a level of the L5 nerve's presacral and the S1 nerve's intrasacral course correlated significantly with HRUS-CSA of the brachial plexus at the interscalene space ($p = 0.041$, $r = 0.57$, $n = 13$), but not with the HRUS-CSA of the brachial plexus

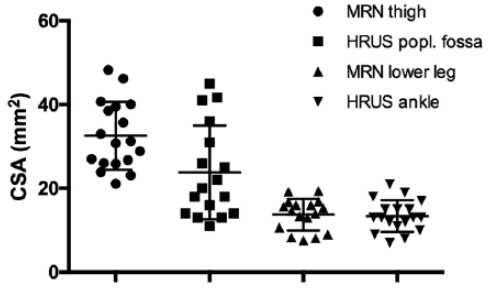

Figure 2. CSA in mm² of the tibial nerve gradually increases from distal to proximal segments of the lower extremities. No correlation between MRN and HRUS-CSA was found for the tibial nerve.
CSA, cross-sectional area; HRUS, high-resonance nerve ultrasound; MRN, magnetic resonance neurography.

at the supraclavicular space ($p = 0.15$, $r = 0.4391$, $n = 13$).

nT2 signal of the lumbrosacral plexus correlated significantly with the CSA of the brachial plexus at the interscalene space ($p = 0.023$, $r = 0.63$, $n = 13$).

HRUS-CSA at the interscalene space did not correlate with the F-wave latency from the median nerve ($p = 0.54$, $r = 0.20$, $n = 11$); neither did HRUS-CSA at the supraclavicular space ($p = 0.33$, $r = 0.31$, $n = 11$) (Table 1).

Correlations with clinical parameters

There were no further significant correlations of the HRUS parameters for each nerve to clinical parameters (ODSS) (Supplementary Table 2). Clinical disease course, MRC scores and disease duration did not correlate with sonographical, electrophysiological or MRN measures.

CSA, nT2 and FA measurements in nonexcitable nerves

In order to detect additional information provided by HRUS and MRN when nerve excitation is not possible or the CMAP is very low, we analysed the CSA, nT2 and FA values for these nerve segments. The tibial nerve of seven patients provided CMAP <1 mV both after distal and proximal stimulation, whereas for the rest of the CIDP patients ($n = 11$) tibial nerves showed mostly demyelinating characteristics in the NCS.

As shown in Table 2, the patients with low tibial CMAP had higher ODSS and longer disease duration (though not statistical significant) than the patients with excitable tibial nerves with demyelinating characteristics. MRN as well as HRUS both depicted a pronounced CSA proximally for these nerves, whereas distally the difference was not significant between the two groups. nT2 signal showed a tendency to higher values for the nonexcitable nerves (nT2 thigh $p = 0.06$), but FA was significantly reduced for these nerves compared to the rest of the excitable nerves.

Discussion

We present a clinical, electrophysiological, sonographical and MRN study examining the complementary role of two neuroimaging methods of the peripheral nervous system in patients with CIDP, and exploiting the significance of CSA increase through correlations with nT2 signal intensity and DTI measures (FA).

Correlation of CSA between HRUS and MRN

To our knowledge no previous studies have performed extensive correlation analyses between MRN- and HRUS-CSA of the peripheral nerves, whereas one study has examined CSA of the brachial plexus with both methods.[16] The maximal CSA values measured with HRUS correlated significantly with maximal CSA-MRN for all nerves measured at the same segment (median, ulnar and radial nerve at the upper arm), as well as for the fibular nerve at the thigh (there, MRN measurements were performed 10–20 cm proximally to the popliteal fossa, HRUS measurements at the popliteal fossa).

Bland–Altmann analyses revealed that the mean bias between these two methods was the lowest for the radial nerve and the highest for the fibular nerve (radial upper arm -0.61 mm² < ulnar upper arm -1.60 mm² < median upper arm -2.4 mm² <

Table 2. Statistical analyses of CSA, T2 and FA values between patients with nonexcitable tibial nerves and demyelinating characteristics in NCS. Nonexcitable nerves have a higher proximal CSA on MRN and HRUS and lower proximal FA values.

	Nonexcitable Mean ± SD (n = 7)	Demyelination Mean ± SD (n = 11)	p value
ODSS	3.8 ± 1.5	2.7 ± 1.1	0.13
Disease duration	5.4 ± 4.4	2.8 ± 1.3	0.3
MRN-CSA thigh	40.6 ± 5.5	27.4 ± 4.3	**0.0003**
HRUS-CSA knee	31.1 ± 12.1	18.3 ± 7.7	**0.03**
MRN-CSA lower leg	16.2 ± 2.5	12.4 ± 3.7	0.1
HRUS-CSA ankle	15.5 ± 3.7	11.5 ± 3.6	0.058
nT2 thigh	1.563 ± 0.28	1.29 ± 0.33	0.06
nT2 lower leg	1.311 ± 0.44	1.286 ± 0.40	0.72
FA thigh	3075 ± 441	4315 ± 777	**0.0019**
FA lower leg	3467 ± 490	4134 ± 483	**0.02**

CSA, cross-sectional area; FA, fractional anisotropy; HRUS, high-resonance nerve ultrasound; MRN, magnetic resonance neurography; nT2, normalized nerve T2-weighted signal; ODSS, overall disability sum score; SD, standard deviation.

fibular thigh −3.26). Furthermore, the MRN measured more frequently a higher CSA for all nerves.

These results point to a good reproducibility of MRN and HRUS measurements at the upper extremity, whereas for nerves with larger CSA the bias was higher and up to 2–3 mm^2.

Two reasons could be proposed for the higher CSA values measured by MRN. First, MRN measured the maximal CSA of the nerves in the study area, whereas in HRUS the maximal CSA was measured at predefined places. A second reason could be that HRUS is able to achieve a perpendicular position for all nerves, whereas the position of the extremities cannot change depending on the examined nerve in MRN so that a tilted position is more probable for all nerves.

For the tibial nerve, our combined MRN-HRUS analyses revealed a high range of variability during its course. MRN values for the tibial portion of the sciatic nerve correlated with MRN tibial CSA values measured 8–12 cm distally to the popliteal fossa, but did not correlate with HRUS tibial CSA values (performed at the popliteal fossa and at the ankle).

Therefore, we conclude that neuroimaging of the tibial nerve requires both methods in order to be complete. On the contrary, HRUS of the nerves on the upper arm and of the fibular nerve in the popliteal fossa correlates with MRN values and therefore HRUS is sufficient for an initial imaging/screening of these nerves in patients with CIDP.

The lumbrosacral plexus can only be imaged with MRN studies. However, our study shows a correlation of the average of the CSAs of the anterior divisions of the spinal nerves L5 and S1 with the interscalene CSA of the brachial plexus, which can be easily monitored with HRUS. The interscalene CSA should therefore be taken into account for further longitudinal studies investigating correlation of clinical and electrophysiological values as a marker of the two most important spinal nerves of the lower extremities.

Correlation of electrophysiological parameters and clinical characteristics

The correlations we found in our study depict the controversies, discussed in the literature until now. Only CSA of the median nerve (HRUS) correlated with CV but not with CMAP, implying that higher CSA correlates with more demyelination for this cohort.

Generally, we propose that sonographical measurements depict a more dynamic situation. The

CSA of the peripheral nerves can change more robustly over time and therefore does not always correlate with NCS studies. CSA in nerve segments with demyelinating NCS correlated with conduction velocity in the study reported by Di Pasquale and colleagues.[17] If NCS characteristics are mixed (axonal and demyelinating), as presented in cohorts with a high variation of ODSS (our study ODSS variation 1–6, study from Di Pasquale and colleagues 1–2), then HRUS-CSA values do not correlate well with NCS studies.[4–6,12,17]

The fact that nonexcitable nerve segments showed a higher CSA both in HRUS and MRN in comparison to the excitable nerve segment of these patients could imply a crucial role of morphological nerve studies in these cases. These nonexcitable segments seem to have retained an increased CSA, although the electrophysiological studies imply at least profound axonal damage. We conclude that the increased CSA provided additional evidence of secondary axonal damage (and not primary axonal damage).

Regarding clinical characteristics (ODSS, disease duration, MRC), we did not find any correlation with CSA values. In our opinion, this could be attributed to the small number of patients in our cohort.

However, patients with low CMAP amplitudes of the tibial nerve (Table 2) did show a nonsignificant trend towards a higher ODSS and a longer disease duration than patients with higher amplitudes, and also had significantly increased proximal CSA-HRUS-MRN values of the tibial nerve as well as significantly decreased FA in proximal nerve segments.

Correlation of nT2 and DTI parameters to HRUS-CSA

In the present study, we introduce for the first time correlations of nerve signal changes to HRUS-CSA measurements.

nT2 signal changes have been reported in CIDP patients and correlate to MRN-CSA measurements, whereas their correlation to electrophysiological and clinical parameters does not seem to be as good as CSA correlation.[8,16] Using multiecho T2-relaxometry, we have recently shown that the physical cause of nT2 increase is an increase of the proton-spin-density q, and not a prolongation of the T2 relaxation time. This increase is mostly caused by an increase of 'bound' intraneural water, tightly restricted by macromolecules or myelin membranes, and not by an increase of free water in the nerve (prolongation of T2 relaxation time), which is the case for symptomatic amyloid neuropathy.[15,18,19]

As described before, DTI is an advanced MRI technique for functional measurement, and depicts microstructural integrity of nervous tissue. FA, as the most commonly used DTI parameter of diffusion, is a biomarker for nerve fibre intensity. Normal peripheral nerves are characterized by high FA values, reflecting the longitudinal organization of cell membranes, whereas FA decrease is considered a quantitative biomarker of nerve tissue damage. Our group described a decreased mean FA of the tibial nerve, which was significantly associated with demyelination.[19]

The majority of publications reporting a HRUS-CSA increase in CIDP have postulated that this correlates with inflammation or nerve oedema. Our study provides, for the first time, proof for a positive correlation of HRUS-CSA values and T2/DTI parameters for our cohort, which support this hypothesis.

The nT2 signal of the ulnar nerve correlated most strongly with HRUS-CSA. HRUS-CSA of the interscalene brachial plexus did not only correlate with the MRN-CSA of L5–S1 roots, but also with the nT2 signal of these roots, confirming the potentially crucial role of this examination in nerve ultrasound studies.

Interestingly, in contrast to nT2, FA of the median nerve as a marker of microstructural integrity correlated strongly with HRUS-CSA and MRN-CSA.

Both measures (nT2 for intraneural water content and FA for microstructural integrity) could be useful biomarkers for prognosis of severity and treatment response; therefore, their correlation to HRUS-CSA offers another tool for the physician treating CIDP patients. It is clear that only histological studies provide a reliable read-out on the mechanism of CSA increase, but we believe that this correlation analysis provides useful markers for future longitudinal MRN and HRUS studies on nerve morphology for CIDP. As described above, HRUS is able to provide a reliable CSA estimation; however, it cannot provide markers

on nerve integrity. The estimation of these parameters and not CSA will be, in our opinion, the future role of MRN in treatment monitoring of CIDP patients.

We conclude that HRUS and MRN should be used as complementary neuroimaging methods in CIDP. HRUS as a cheap and easily accessible method could be used as an initial screening tool for CSA increase of all peripheral nerves and the brachial plexus. However, neuroimaging of the proximal segments of the tibial nerve and the lumbrosacral plexus requires MRN measurements. Furthermore, MRN is the only method able to provide signal alteration markers such as nT2 and FA, which could be useful for treatment monitoring.

Neuroimaging studies on larger cohorts including longitudinal examinations will hopefully shed light on the secrets of peripheral nerve pathology and contribute to an optimal characterization of CIDP patients in the following years.

Author contributions

Kalliopi Pitarokoili: study design, acquisition of data, analysis and interpretation of data, drafting/revising the manuscript for content.
Moritz Kronlage: acquisition of data, analysis and interpretation of data, drafting/revising the manuscript for content.
Philipp Bäumer: analysis and interpretation of data, drafting/revising the manuscript for content.
Daniel Schwarz: analysis and interpretation of data, drafting/revising the manuscript for content.
Ralf Gold: study design, drafting/revising the manuscript for content.
Martin Bendszus: study design, study supervision, drafting/revising the manuscript for content.
Min-Suk Yoon: study design, analysis and interpretation of data, revising the manuscript for content.

Conflict of interest statement

Kalliopi Pitarokoili received travel grants from Biogen Idec and Bayer Schering and speaker's honoraria from Biogen Idec, Bayer Schering and Novartis.
Moritz Kronlage, Phillip Bäumer and Daniel Schwarz report no disclosures.
Ralf Gold received speaker's and board honoraria from Baxter, Bayer Schering, Biogen Idec, CLB Behring, Genzyme, Merck Serono, Novartis, Stendhal, Talecris and TEVA, all unrelated to the current study. His department received grant support from Bayer Schering, Biogen Idec, Genzyme, Merck Serono, Novartis and TEVA, all unrelated to the current study.
Martin Bendszus received grants and personal fees from Novartis, Guerbet and Codman; personal fees from Vascular Dynamics, Roche, TEVA, Springer, Boehringer and Bayer Vital; and grants from Siemens, Hopp Foundation, Stryker, Medtronic and DFG, all unrelated to the current study.
Min-Suk Yoon has received speaker's honoraria from CSL Behring, unrelated to the current study.

Funding

This research received no specific grant from any funding agency in the public, commercial or not-for-profit sectors.

Supplemental Material

Supplementary material for this article is available online.

References

1. National Clinical Guideline Centre (UK). *Multiple sclerosis: management of multiple sclerosis in primary and secondary care*. London: National Institute for Health and Care Excellence (UK), 2014.

2. Van den Bergh PY, Hadden RD, Bouche P, *et al.*; European Federation of Neurological Societies; Peripheral Nerve Society. European Federation of Neurological Societies/Peripheral Nerve Society guideline on management of chronic inflammatory demyelinating polyradiculoneuropathy: report of a joint task force of the European Federation of Neurological Societies and the Peripheral Nerve Society: first revision. *Eur J Neurol* 2010; 17: 356–363.

3. Kerasnoudis A, Pitarokoili K, Behrendt V, *et al*. Nerve ultrasound score in distinguishing chronic from acute inflammatory demyelinating polyneuropathy. *Clin Neurophysiol* 2014; 125: 635–641.

4. Shibuya K, Sugiyama A, Ito S, *et al*. Reconstruction magnetic resonance neurography in chronic inflammatory demyelinating polyneuropathy. *Ann Neurol* 2015; 77: 333–337.

5. Pitarokoili K, Schlamann M, Kerasnoudis A, *et al*. Comparison of clinical, electrophysiological, sonographic and MRI features in CIDP. *J Neurol Sci* 2015; 357: 198–203.

6. Grimm A, Rattay TW, Winter N, *et al*. Peripheral nerve ultrasound scoring systems: benchmarking and comparative analysis. *J Neurol* 2017; 264: 243–253.
7. Goedee HS, van der Pol WL, van Asseldonk JH, *et al*. Diagnostic value of sonography in treatment-naive chronic inflammatory neuropathies. *Neurology* 2017; 88: 143–151.
8. Baumer P, Weiler M, Bendszus M, *et al*. Somatotopic fascicular organization of the human sciatic nerve demonstrated by MR neurography. *Neurology* 2015; 84: 1782–1787.
9. Kerasnoudis A, Pitarokoili K, Behrendt V, *et al*. Increased cerebrospinal fluid protein and motor conduction studies as prognostic markers of outcome and nerve ultrasound changes in Guillain–Barré syndrome. *J Neurol Sci* 2014; 340: 37–43.
10. Kronlage M, Pitarokoili K, Schwarz D, *et al*. Diffusion tensor imaging in chronic inflammatory demyelinating polyneuropathy: diagnostic accuracy and correlation with electrophysiology. *Invest Radiol* 2017; 52: 701–707.
11. Yoon MS, Chan A and Gold R. Standard and escalating treatment of chronic inflammatory demyelinating polyradiculoneuropathy. *Ther Adv Neurol Disord* 2011; 4: 193–200.
12. Kerasnoudis A, Pitarokoili K, Haghikia A, *et al*. Nerve ultrasound protocol in differentiating chronic immune-mediated neuropathies. *Muscle Nerve* 2016; 54: 864–871.
13. Merkies IS, Schmitz PI, van der Meché FG, *et al*.; Inflammatory Neuropathy Cause and Treatment (INCAT) Group. Clinimetric evaluation of a new overall disability scale in immune mediated polyneuropathies. *J Neurol Neurosurg Psychiatry* 2002; 72: 596–601.
14. Stöhr M and Pfister R. *Clinical electromyography and neurography*. 6th ed. Stuttgart: Koehlhammer, 2014: p.215.
15. Kronlage M, Bäumer P, Pitarokoili K, *et al*. Large coverage MR neurography in CIDP: diagnostic accuracy and electrophysiological correlation. *J Neurol* 2017; 264: 1434–1443.
16. Goedee HS, Jongbloed BA, van Asseldonk JH, *et al*. A comparative study of brachial plexus sonography and magnetic resonance imaging in chronic inflammatory demyelinating neuropathy and multifocal motor neuropathy. *Eur J Neurol* 2017; 24: 1307–1313.
17. Di Pasquale A, Morino S, Loreti S, *et al*. Peripheral nerve ultrasound changes in CIDP and correlations with nerve conduction velocity. *Neurology* 2015; 84: 803–809.
18. Tanaka K, Mori N, Yokota Y, *et al*. MRI of the cervical nerve roots in the diagnosis of chronic inflammatory demyelinating polyradiculoneuropathy: a single-institution, retrospective case–control study. *BMJ Open* 2013; 3: e003443.
19. Kollmer J, Hund E, Hornung B, *et al*. In vivo detection of nerve injury in familial amyloid polyneuropathy by magnetic resonance neurography. *Brain* 2015; 138 (Pt. 3): 549–562.